



## Scanning Josephson Tunneling Microscopy of Single-Crystal $\text{Bi}_2\text{Sr}_2\text{CaCu}_2\text{O}_{8+\delta}$ with a Conventional Superconducting Tip

Hikari Kimura,<sup>1,2</sup> R. P. Barber, Jr.,<sup>3</sup> S. Ono,<sup>4</sup> Yoichi Ando,<sup>5</sup> and R. C. Dynes<sup>1,2,\*</sup>

<sup>1</sup>*Department of Physics, University of California, Berkeley, California 94720, USA*

<sup>2</sup>*Materials Sciences Division, Lawrence Berkeley National Lab., Berkeley, California 94720, USA*

<sup>3</sup>*Department of Physics, Santa Clara University, Santa Clara, California 95053, USA*

<sup>4</sup>*Central Research Institute of Electric Power Industry, Komae, Tokyo 201-8511, Japan*

<sup>5</sup>*The Institute of Scientific and Industrial Research, Osaka University, Ibaraki, Osaka 567-0047, Japan*

(Received 15 April 2008; revised manuscript received 26 May 2008; published 18 July 2008)

We have performed both Josephson and quasiparticle tunneling in vacuum tunnel junctions formed between a conventional superconducting scanning tunneling microscope tip and overdoped  $\text{Bi}_2\text{Sr}_2\text{CaCu}_2\text{O}_{8+\delta}$  single crystals. A Josephson current is observed with a peak centered at a small finite voltage due to the thermal-fluctuation-dominated superconducting phase dynamics. Josephson measurements at different surface locations yield local values for the Josephson  $I_C R_N$  product. Corresponding energy gap measurements were also performed and a surprising inverse correlation was observed between the local  $I_C R_N$  product and the local energy gap.

DOI: [10.1103/PhysRevLett.101.037002](https://doi.org/10.1103/PhysRevLett.101.037002)

PACS numbers: 74.40.+k, 74.25.Dw, 74.50.+r, 74.72.Hs

Remarkable scanning tunneling microscopy (STM) studies on the high- $T_C$  superconducting cuprate (HTSC),  $\text{Bi}_2\text{Sr}_2\text{CaCu}_2\text{O}_{8+\delta}$  (BSCCO) reveal spectral and energy gap inhomogeneities [1,2], periodic electronic structure in the superconducting (SC) state [3] and structure inside vortex cores [4] as well as in the pseudogap state at temperatures above  $T_C$  [5]. In these experiments the energy gap  $\Delta$  is taken to be half the energy separation between the quasiparticle (QP) coherence peaks as observed in  $dI/dV$  spectra. The appearance of  $\Delta$  has also been observed at a temperature  $T^*$  above  $T_C$  with constant ratio  $2\Delta/k_B T^*$  [6]. The identification of  $\Delta$  becomes ambiguous, however, in heavily underdoped BSCCO where the observed  $dI/dV$  no longer has well-defined sharp coherence peaks [7,8]. Two important issues raised by these complex results are (i) whether the SC order parameter of BSCCO has spatial variation, and (ii) how the SC ground state correlates with the QP excited states ( $\Delta$ ). These uncertainties motivate a direct probe of the SC pair wave function. Normal-metal STM studies reveal only the QP excitation spectrum. However, an STM with a SC tip is a local Josephson probe and can, in principle, access the SC pair wave function directly on a length scale smaller than or comparable to the SC coherence length,  $\xi$ .

Between conventional superconductors the Josephson  $I_C R_N$  product is a directly measurable quantity uniquely determined by the specific materials in the Josephson junction, where  $I_C$  is the critical current and  $R_N$  the junction normal-state resistance. Furthermore, this parameter is directly linked to both the SC order parameter amplitude and the energy gaps  $\Delta_{\text{BCS}}$  of the materials through the BCS relationship. Josephson studies using a SC-STM on conventional superconductors were validated by the good agreement between the measured  $I_C R_N$  and BCS theory [9,10]. For HTSCs, on the other hand, there is no estab-

lished theory to relate  $I_C R_N$  with  $\Delta$  derived from the QP excitation spectrum.  $I_C R_N$  measurements on BSCCO using a SC-STM should, however, both prove the existence and yield the amplitude of the BSCCO pair wave function that couples to the conventional SC tip. Because of the spatial resolution of an STM, this measurement could reveal useful new information regarding inhomogeneity in the superconductivity of BSCCO.

The observation of strong  $c$ -axis Josephson coupling in planar  $\text{Pb-YBa}_2\text{Cu}_3\text{O}_{7-\delta}$  (YBCO) single-crystal Josephson junctions can be explained by an  $s$ -wave component in the order parameter of YBCO induced by an orthorhombic distortion [11]. Although the crystallographic symmetry of BSCCO makes  $s$ - and  $d$ -wave mixing less likely, Josephson coupling between conventional superconductors and BSCCO in planar junctions has been observed [12,13].  $I_C R_N$  values for these junctions (Nb- or Pb-BSCCO) ranged from 1  $\mu\text{V}$  to 10  $\mu\text{V}$ , indicating that the  $s$  component is about 3 orders of magnitude smaller than the  $d$ -component. Because  $I_C R_N$  was measured in macroscopic junctions, any strong local inhomogeneities were obscured and meaningful comparisons with an inhomogeneous  $\Delta$  could not be made. It is, therefore, very important to locally probe the order parameter in this strongly inhomogeneous material using Josephson tunneling.

In this Letter we report on direct measurements of the SC ground state of overdoped BSCCO using a SC-STM. Local measurements of both  $I_C R_N$  and  $\Delta$  were performed.  $I_C R_N$  as a function of  $\Delta$  tends to decrease as  $\Delta$  increases. This result is unexpected from BCS theory and consistent with the phase fluctuation model for HTSCs proposed by Emery and Kivelson [14].

The novel feature of our SC-STM is a SC tip (Pb with a Ag capping layer) in close proximity to a SC sample to form a superconductor-insulator-superconductor (S/I/S)

tunnel junction [15]. The operation of this SC-STM has been demonstrated with the observation of Josephson tunneling between the tip and both SC Pb films [9] and SC NbSe<sub>2</sub> [10]. The signature Josephson response of the SC-STM differs from that of typical low  $R_N$  planar S/I/S devices. Because of the experimental base temperature ( $T = 2.1$  K) and large  $R_N$  associated with an STM, the Josephson binding energy,  $E_J$ , which couples the separate SC ground states is smaller than  $k_B T$ . For example with an STM resistance of 50 k $\Omega$ ,  $E_J/k_B$  is roughly 1 K. Also for ultrasmall tunnel junctions, the Coulomb charging energy,  $E_C$  can be large. We estimate the capacitance,  $C$ , of the STM junction formed between the conical tip apex and the sample surface to be about 1 fF.  $E_C = e^2/2C$  is therefore of order 1 K: comparable with  $E_J$ , but smaller than  $k_B T$ . Furthermore the time scale of an electron tunneling in the STM junction is much shorter than  $\hbar/E_C$ , so that the electron is swept away long before the charging effects become relevant. Because  $k_B T$  is the dominant energy, the phase difference of the two superconductors,  $\phi$ , is not locked in a minimum of the sinusoidal  $E_J$  vs  $\phi$  washboard potential, but is thermally excited and diffusive. Near zero bias voltage the observed Josephson current is therefore dependent on the bias due to the dissipative phase motion. The experimental data for a Pb film has been explained by a phase diffusion model first proposed by Ivanchenko-Zilberman [16] and later by others [17,18]. The current-voltage ( $I$ - $V$ ) characteristics are described by

$$I(V) = \frac{I_C^2 Z_{\text{env}}}{2} \frac{V}{V^2 + V_p^2}, \quad (1)$$

where the peak in the Josephson current appears at a voltage  $V_p = (2e/\hbar)Z_{\text{env}}k_B T_n$ . In this model we can consider the thermal fluctuations as Johnson noise generated by a resistor  $Z_{\text{env}}$  at temperature  $T_n$ ; both parameters depend only on the experimental set-up. The observed  $I$ - $V$  characteristics for Pb/I/Pb STM Josephson junctions near zero bias with various  $R_N$  are fitted to Eq. (1) with two parameters,  $V_p$  and  $I_C$ . This analysis yields a plot of  $I_C/\sqrt{k_B T_n}/e$  vs  $G_N = 1/R_N$  and is expected to be linear with zero intercept (no  $I_C$  at infinite  $R_N$ ) and a slope equal to  $I_C R_N/\sqrt{k_B T_n}/e$ . Using  $I_C R_N(\text{Pb/I/Pb}) = 1.671$  mV [19] known from the Ambegaokar-Baratoff formula [20] and substituting it into the slope of the linear data fit, we can determine  $T_n$  and  $Z_{\text{env}}$  for our STM Josephson junctions. Current values of these parameters are  $15.9 \pm 0.1$  K and  $279 \pm 9$   $\Omega$ , respectively.

Using our well-characterized SC-STM, we have studied overdoped BSCCO single crystals with  $T_C$  values of 76, 79, and 81 K. Samples are cleaved in ultrahigh vacuum and cooled to  $T = 2.1$  K. Because of the thick Pb layer used in our SC tip fabrication, we rarely observe atomic resolution images. However we can easily locate step edges and isolate flat surfaces where all the present data were measured. We first observe the  $dI/dV$  spectrum at a particular

surface point on sample 1 ( $T_C = 79$  K) to measure the BSCCO energy gap  $\Delta$  (black line in the inset of Fig. 1). We use standard lock-in techniques with 1 KHz modulation on the bias voltage and an  $R_N \sim 500$  M $\Omega$ . Although a simplification of a more complex structure, we use the same definition for  $\Delta$  as in previous works in order to make comparisons. In the main frame we plot the  $I$ - $V$  characteristics at lower bias and lower  $R_N$ . A low leakage current below the Pb gap confirms high quality vacuum tunnel junctions. Further decreasing  $R_N$  increases the QP tunneling probability and finally the thermally fluctuated Josephson currents are observed when  $E_J$  is comparable to  $k_B T_n$ . The QP background inside the Pb gap is much larger than that of Pb/I/Pb STM Josephson junctions because of the gaplessness of the local density of states (LDOS) of BSCCO.

Figure 2(a) displays a close-up view of the  $I$ - $V$  characteristics near zero bias, clearly showing that the SC Pb tip was Josephson coupled to the BSCCO. The averaged QP background is represented by the red line in Fig. 2(b). Figure 2(c) shows the contributions from the thermally fluctuated Josephson current after subtracting the QP background of Fig. 2(b) from the  $I$ - $V$  curves of Fig. 2(a). The data in Fig. 2(c) are shown as lines and the best fits to Eq. (1) are represented by the symbols. These good fits convince us that we have observed the pair current between a conventional ( $s$ -wave) SC Pb tip and overdoped BSCCO, suggesting that the BSCCO does not have a pure  $d$ -wave order parameter. In addition, the  $dI/dV$  represented by the red line in the inset of Fig. 1 was observed after low  $R_N$  measurements in Fig. 2. The LDOS was changed significantly during the measurements; and the QP coherence

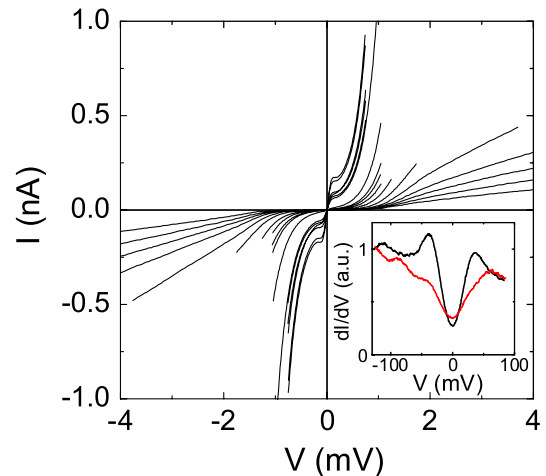


FIG. 1 (color online).  $I$ - $V$  characteristics of Pb/I/overdoped BSCCO ( $T_C = 79$  K) STM Josephson junctions at  $T = 2.1$  K. The Pb gap is clearly seen around  $V = 1.4$  mV. Inset:  $dI/dV$  spectrum (black line) measured before low  $R_N$  measurements, showing sharp coherence peaks with  $\Delta = 37$  meV.  $dI/dV$  measured after low  $R_N$  measurements (red line) indicates an LDOS change due to the high current density.

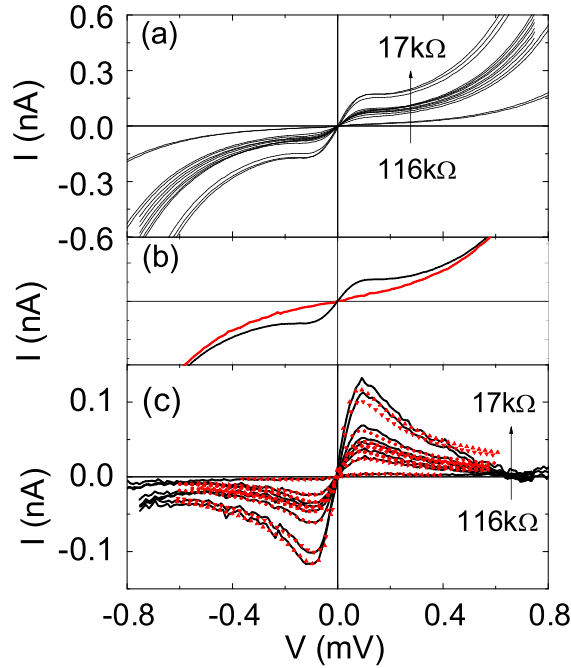


FIG. 2 (color online). (a) Low bias  $I$ - $V$  characteristics of Fig. 1 for various  $R_N$  at  $T = 2.1$  K. (b) Averaged  $I$ - $V$  characteristic near zero bias for quasiparticle background (red line). One of the observed  $I$ - $V$  curves is shown by the black line. (c) Thermally fluctuated Josephson currents peaked at  $V_p$  as derived by subtracting quasiparticle background [Fig. 2(b)] from the  $I$ - $V$  curves [Fig. 2(a)]. The data are represented by the lines and the symbols represent two-parameter fits to the phase diffusion model.

peaks have disappeared, perhaps due to the high current density of the measurements at the highest conductances studied. This  $dI/dV$  resembles those previously observed in heavily underdoped BSCCO [6–8], and in the pseudogap state at temperatures above  $T_C$  [21]. It is also similar to the  $dI/dV$  spectra observed by others on surfaces which were altered by scanning with large tunnel currents [22]. It is important to note that LDOS changes were observed only when measurements were made with  $R_N$  below  $30\text{ k}\Omega$ . In order to avoid this effect, most of the data presented here were obtained with  $R_N$  ranging from  $30\text{ k}\Omega$  to  $100\text{ k}\Omega$ .

A fit to each  $I$ - $V$  curve in Fig. 2(c) generates a single data point in the plot shown in Fig. 3. As  $G_N$  is increased ( $R_N$  is reduced) the observed  $I_C$  increases ( $E_J$  increases). Using the previously determined  $T_n$  and  $Z_{\text{env}}$  and the slope of the linear fit shown in Fig. 3, we find  $I_C R_N$  at this surface point to be  $335\text{ }\mu\text{V}$ . It is important to note that low  $R_N$  measurements ( $R_N$  below  $\sim 300\text{ k}\Omega$ ) on BSCCO increase the low frequency noise on the tunnel current. This noise appears to be induced locally on the BSCCO and not from the environment or electronics. We assure that we have not affected the tip during the measurements by verifying that the Pb gap is always reproduced and exponential decay of

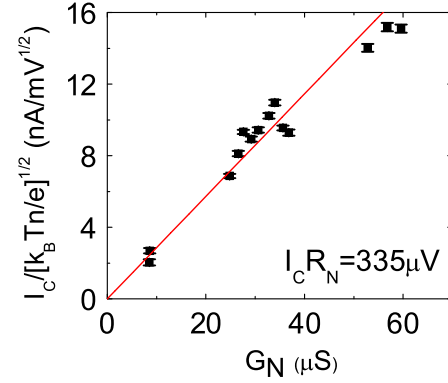


FIG. 3 (color online). Plot of  $I_C / \sqrt{k_B T_n / e}$  vs  $G_N$ . The slope is equal to  $I_C R_N / \sqrt{k_B T_n / e}$ . Using the fitted slope and substituting the previously determined  $T_n$ , the Josephson product at this surface point is found to be  $I_C R_N = 335\text{ }\mu\text{V}$ .

the tunnel current vs the tip-sample distance is also observed after low  $R_N$  measurements.

Figure 4 summarizes Josephson  $I_C R_N$  product vs  $\Delta$  measurements for four overdoped samples with each data point taken at locations roughly  $10\text{ }\text{\AA}$  apart. Although there is scatter in the observed  $I_C R_N$  values for a given  $\Delta$ , this figure clearly indicates the nanometer scale inhomogeneities in both  $I_C R_N$  and  $\Delta$ . The reason for the scatter from experiment to experiment is under investigation. The notable result in Fig. 4 is that  $I_C R_N$  tends to be a maximum when  $\Delta$  is between  $40$  and  $45\text{ meV}$ , and the trend is for it to decrease or become zero as  $\Delta$  increases or decreases from this maximal point.

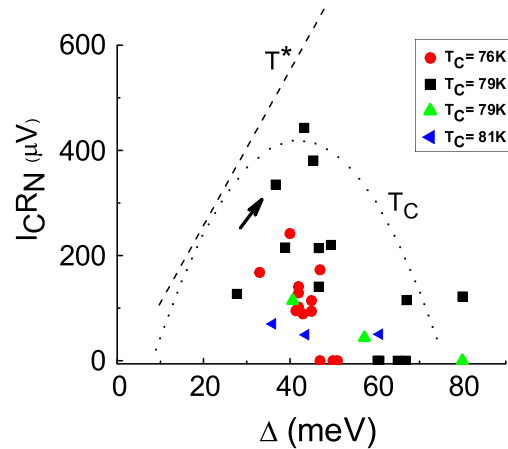


FIG. 4 (color online).  $I_C R_N$  as a function of  $\Delta$ . Each data point represents a separate measurement from a different location over 4 different samples. The  $I_C R_N$  value derived from Fig. 3 is one of the black square symbols denoted with an arrow. All other points are derived similarly.  $I_C R_N$  appears to be a maximum for  $\Delta$  between  $40$  and  $45\text{ meV}$ , while it decreases for larger and smaller  $\Delta$ . Sketches of  $T_C$  and  $T^*$  from the Emery-Kivelson model are shown by dotted and dashed lines, respectively. The vertical scale for the model curves is arbitrary.

We interpret these results within the framework of the phase diagram for HTSCs proposed by Emery and Kivelson (EK model) [14]. In this picture  $T_C$  vs hole doping,  $\delta$ , in the SC region has a dome shape with the maximum  $T_C$  at  $\delta \sim 0.16$ . Changing  $\delta$  from this value results in a  $T_C$  decrease. Another parameter,  $T^*$  is described as the temperature below which a gap in the QP spectrum is formed, but without long-range phase coherence.  $T^*$  continues to rise as  $\delta$  decreases and  $T_C$  decreases.

In order to overlay this phase diagram on our Fig. 4, we make two assumptions. First, we note that  $T^*$  decreases monotonically as  $\delta$  increases. Using previous results that  $\Delta/T^*$  is observed to remain constant for optimally doped and overdoped BSCCO [6], we can transform the model's  $\delta$ -axis into the  $\Delta$ -axis in our Fig. 4. Now  $T^*$  monotonically increases and the dome-shaped region is simply flipped horizontally as shown when plotted vs  $\Delta$ . Second, we assume that parameters for each sample location are correlated with the locally measured  $\Delta$  and therefore the corresponding doping which produces samples with the same average behavior. For example, Fig. 4 indicates that  $I_C R_N$  is maximized at a gap value of  $40 \sim 45$  meV, the average  $\Delta$  typically observed in optimally-doped BSCCO (corresponding to the highest  $T_C$  samples).  $I_C R_N$  decreases as  $\Delta$  becomes larger or smaller than this value, and therefore follows a trend similar to that of the  $T_C$  curve in the model. It is important to reiterate that for any given sample, we observed inhomogeneities both in  $\Delta$  and  $I_C R_N$  as a function of location.

From our results we correlate the observed  $I_C R_N$  with the amplitude of the SC order parameter  $|\Psi|$  as well as with the  $T_C$  of BSCCO via the EK model phase diagram. These three quantities ( $I_C R_N$ ,  $|\Psi|$  and  $T_C$ ) decrease (smaller superfluid density) as  $\Delta$  increases and anticorrelate with  $T^*$ . This inverse relation between  $I_C R_N$  and  $\Delta$  in BSCCO is an unconventional result because in the BCS model  $\Delta_{BCS}$ ,  $I_C R_N$ ,  $|\Psi|$  and  $T_C$  are all correlated. We observe a more conventional behavior in the overdoped (amplitude dominated) side of the phase diagram. Here both  $T_C$  and  $\Delta$  decrease as  $\delta$  is increased above 0.16. In this regime (the averaged  $\Delta \leq 40$  meV),  $T^*$  and  $I_C R_N$  closely relate to  $\Delta$  so that  $I_C R_N$ ,  $|\Psi|$ ,  $T_C$  and  $T^*$  all behave similarly.

Another possible framework for discussing our results is the two-gap scenario [23]. In the underdoped regime, this picture conjectures that the large gap observed in the pseudogap phase is distinct from the genuine superconducting gap that tracks  $T_C$ . Although consistent with our  $I_C R_N$  measurements, we do not observe the second gap directly. Since the results in Fig. 4 represent measurements of both  $I_C R_N$  and  $\Delta$  averaged over momentum space, we are unable to do the same local comparison to address this alternate model.

In summary, we have observed the thermally fluctuated Josephson current for  $c$ -axis tunneling between a SC Pb tip and overdoped BSCCO single crystals. To our knowledge this is the first local Josephson measurement along the  $c$  axis between  $s$ - and  $d$ -wave superconductors. Probing both  $I_C R_N$  and  $\Delta$  over the surface indicates an anticorrelation between the Josephson coupling and  $\Delta$ . This result is consistent with the EK phase fluctuation model for a low superfluid density superconductor.

The authors acknowledge assistance and helpful conversations with Mike Crommie, John Clarke, and Ofer Naaman. We thank Paul Reichardt and Darin Kinion for the cryogenic microwave filter design and the Berkeley Physics Machine shop for expert technical assistance. The work in Berkeley was supported by DOE Grant No. DE-FG02-05ER46194. S.O. was supported by KAKENHI No. 20740213 and Y. A. by KAKENHI No. 19674002.

---

\*rdynes@physics.berkeley.edu

- [1] S. H. Pan *et al.*, Nature (London) **413**, 282 (2001).
- [2] K. M. Lang *et al.*, Nature (London) **415**, 412 (2002).
- [3] J. E. Hoffman *et al.*, Science **297**, 1148 (2002).
- [4] J. E. Hoffman *et al.*, Science **295**, 466 (2002).
- [5] M. Vershinin *et al.*, Science **303**, 1995 (2004).
- [6] K. K. Gomes *et al.*, Nature (London) **447**, 569 (2007).
- [7] K. McElroy *et al.*, Phys. Rev. Lett. **94**, 197005 (2005).
- [8] J. W. Alldredge *et al.*, Nature Phys. **4**, 319 (2008).
- [9] O. Naaman, W. Teizer, and R. C. Dynes, Phys. Rev. Lett. **87**, 097004 (2001).
- [10] O. Naaman, R. C. Dynes, and E. Bucher, Int. J. Mod. Phys. B **17**, 3569 (2003).
- [11] A. G. Sun *et al.*, Phys. Rev. Lett. **72**, 2267 (1994).
- [12] M. Möhle and R. Kleiner, Phys. Rev. B **59**, 4486 (1999).
- [13] I. Kawayama *et al.*, Physica (Amsterdam) **325C**, 49 (1999).
- [14] V. J. Emery and S. A. Kivelson, Nature (London) **374**, 434 (1995).
- [15] O. Naaman, W. Teizer, and R. C. Dynes, Rev. Sci. Instrum. **72**, 1688 (2001).
- [16] Yu. M. Ivanchenko and L. A. Zil'berman, Zh. Eksp. Teor. Fiz. **55**, 2395 (1968) [Sov. Phys. JETP **28**, 1272 (1969)].
- [17] G.-L. Ingold, H. Grabert, and U. Eberhardt, Phys. Rev. B **50**, 395 (1994).
- [18] Y. Harada, H. Takayanagi, and A. A. Odintsov, Phys. Rev. B **54**, 6608 (1996).
- [19] We use  $\Delta_{Pb} = 1.35$  mV and include a factor of 0.788 due to strong phonon coupling in Pb.
- [20] V. Ambegaokar and A. Baratoff, Phys. Rev. Lett. **10**, 486 (1963).
- [21] C. Renner *et al.*, Phys. Rev. Lett. **80**, 149 (1998).
- [22] C. Howald, P. Fournier, and A. Kapitulnik, Phys. Rev. B **64**, 100504(R) (2001).
- [23] W. S. Lee *et al.*, Nature (London) **450**, 81 (2007).